

Grain Growth and the Puzzle of its Stagnation in Thin Films: A Detailed Comparison of Experiments and Simulations

Katayun Barmak^{1,a}, Eva Eggeling^{2,b}, Richard Sharp^{3,c}, Scott Roberts^{1,d},
Terry Shyu^{1,e}, Tik Sun^{4,f}, Bo Yao^{4,g}, Shlomo Ta'asan^{3,h},
David Kinderlehrer^{3,i}, Anthony Rollett^{1,j}, and Kevin Coffey^{4,k}

¹Materials Research Science and Engineering Center and the Department of Materials Science and Engineering, Carnegie Mellon University, 5000 Forbes Avenue, Pittsburgh, PA 15213, USA

²Fraunhofer Austria Research GmbH, 8010 Graz, Austria

³Materials Research Science and Engineering Center and the Department of Mathematical Sciences, Carnegie Mellon University, 5000 Forbes Avenue, Pittsburgh 15213, USA

⁴Advanced Materials Processing and Analysis Center, University of Central Florida, 4000 Central Florida Boulevard, Orlando, FL 32816, USA

^akatayun@andrew.cmu.edu, ^beva.eggeling@fraunhofer.at, ^crwsharp@cmu.edu, ^dsr2e@cmu.edu, ^etshyu@andrew.cmu.edu, ^fti857626@pegasus.cc.ucf.edu, ^gbo555252@pegasus.cc.ucf.edu, ^hshlomo@andrew.cmu.edu, ⁱdavidk@cmu.edu, ^jrollett@andrew.cmu.edu, ^kkrcoffey@mail.ucf.edu

Keywords: Thin film grain growth, grain growth stagnation, grain growth simulation, isotropic and anisotropic grain boundary energy, grain boundary grooving, solute drag, triple junction drag.

Abstract. We revisit grain growth and the puzzle of its stagnation in thin metallic films. We bring together a large body of experimental data that includes the size of more than 30,000 grains obtained from 23 thin film samples of Al and Cu with thicknesses in the range of 25 to 158 nm. In addition to grain size, a broad range of other metrics such as the number of sides and the average side class of nearest neighbors is used to compare the experimental results with the results of two dimensional simulations of grain growth with isotropic boundary energy. In order to identify the underlying cause of the differences between these simulations and experiments, five factors are examined. These are (i) surface energy and elastic strain energy reduction, (ii) anisotropy of grain boundary energy, and retarding and pinning forces such as (iii) solute drag, (iv) grain boundary grooving and (v) triple junction drag. No single factor provides an explanation for the observed experimental behavior.

Introduction

Nanoscale metallic conductors are known to have significantly higher resistivity over their bulk counterparts, a phenomenon known as the classical size effect and first noted by J. J. Thomson in 1901.[1] This effect scales with the conduction electron mean free path, which is approximately 39 nm for Cu at room temperature. The mitigation of this resistivity increase for Cu interconnects has been identified as a “Grand Challenge” problem in the International Technology Roadmap for Semiconductors (ITRS)[2] and has motivated many recent studies. In one such study, Cu film grain size was quantified for a statistically significant population of grains, and it was shown that grain boundary scattering provides the most significant contribution to the observed resistivity increase.[3] The obvious solution for mitigating the resistivity size effect is then to grow the grains. However, it has long been observed that upon post-deposition annealing, grain growth stagnates when the grain size in the plane of the film is 2-4 times the film thickness.[4] It is this puzzle of grain growth stagnation that we address in this paper. A large body of experimental data is compared with the results of two dimensional simulations of grain growth with isotropic boundary energy. This comparison is used to highlight not only where experiments and simulations disagree but also where they show (surprisingly) similar behavior. The paper then examines the various

causes that have been proposed for the observed differences between experiments and simulations. These include driving forces other than grain boundary energy reduction, anisotropy of grain boundary energy, and the presence of retarding and pinning forces such as solute drag, grain boundary grooving and triple junction drag.

Experiment and Simulation

The details of film preparation and characterization can be found elsewhere [3, 5, 6]. Briefly, Al films, with thicknesses of 25, 30 and 100 nm were prepared by sputter deposition. The target purity for the 25 and 100 nm thick films was 99.99%, and the films were deposited onto oxidized Si (100) substrates with 100 nm of thermally grown SiO₂. The total content of the metallic impurities in the sputtering target was 5.6 ppm by weight, of which 3.0 ppm was Fe (equal to 1.45 atomic ppm of Fe). The Si content was 1.8 ppm, and that of the non-metallic impurities H, N, O, and P was 17.5 ppm. The target purity for the 30 nm thick Al film is not known. This film was deposited onto a single crystal of salt. The 25 and 100 nm-thick Al films were annealed at 400°C. The 30 nm-thick Al film was annealed at 450°C. Fifteen samples of SiO₂/Cu/SiO₂ thin films were prepared on Si (100) substrates with 150 nm of thermally grown SiO₂. Prior to film deposition, the substrates were RF sputter cleaned and cooled to -40°C by contact with a liquid nitrogen cooled Cu plate. An underlayer of 20 nm of SiO₂ was RF sputter deposited prior to the Cu film deposition and a 20 nm SiO₂ overlayer was subsequently similarly deposited to form the SiO₂/Cu/SiO₂ structure. The Cu layers were deposited by DC sputter deposition from Cu targets of high purity (99.9999%). The film thicknesses were in the range of 27 to 158 nm. Annealing treatments of 150°C and 600°C for 30 minutes (in a tube furnace) and 400°C for 6 seconds (in a rapid thermal annealing furnace) were used to produce different grain sizes. The annealing ambient for the all the films (Al and Cu) was Ar-3, 4 or 5% H₂. Measurement of film grain size, number of sides and side class of nearest neighbors was done from hand traced boundary networks of images obtained by transmission electron microscopy.

Two-dimensional grain growth simulations were done using a boundary tracking model termed the partial differential equation (PDE) model. Additional details of the simulation procedure are given elsewhere.[7] In the PDE model, the evolution of the grain boundary network is curvature driven, with the Herring condition of force balance imposed at triple junctions. Both isotropic boundary energy and a simplified-anisotropic boundary energy function, in the form of $\sigma = 1 + \varepsilon \sin^2 \theta$ with $\varepsilon = 0.125$ and θ as the misorientation angle across the grain boundary were used in the simulations. The PDE simulations also allowed the impact of triple junction drag on grain growth to be examined. For the case of no drag, the position of the triple junction is determined completely and instantaneously by the positions of the three intersecting boundaries. For the case where triple junction drag is present, the triple junction has a finite velocity, and the lower the velocity, the higher is the drag. A series of 17 triple junction drag parameters in the range of 0.1 (high drag) to 50 (low drag) were used.

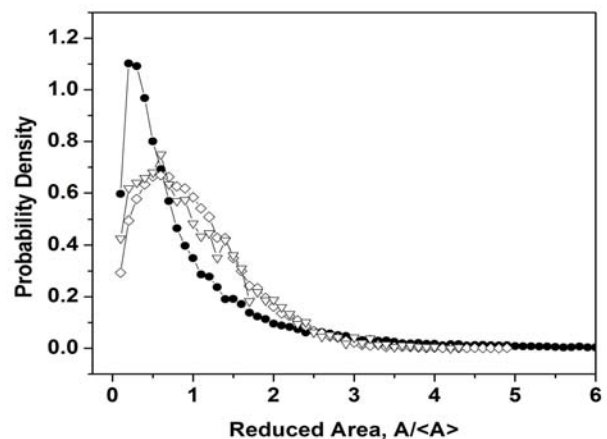


Fig. 1 – Probability densities for reduced grain area for the experimental data for Al and Cu films (filled circles), for two dimensional simulations with isotropic boundary energy (open diamonds), and two dimensional simulations with anisotropic boundary energy (open inverted triangles).

The metrics used for comparison of experiments and simulation were grain size (as grain area or as the diameter of a circle with area equal to the mean grain area), number of sides, side class of nearest neighbors (i.e., average number of sides of the nearest neighbors of grains with a given number of sides), and combined geometry-topology metrics such as the size of grains with a given number of sides.

Results

For the 100 nm thick Al film, grain size was measured as a function of annealing time at 400 °C. The as-deposited film had a grain size of 85 nm. The size increased to 104 nm after 0.5 h of annealing. The stagnation in grain growth at a grain size of approximately 168 nm occurred at ≥ 1 hour of annealing. Grain size was also measured for given side classes between 3 and 9. The stagnation in size was observed for all these classes. For the Cu films, grain size was not measured as a function of time. However, the maximum grain size that was achieved did not exceed three times the film thickness, independent of annealing temperature. This grain size to thickness ratio is thus within the range associated with stagnation.[4]

The probability density for the reduced (or the relative) grain area, $A/\langle A \rangle$ is shown in Fig. 1 for 21 out of the 23 films studied, namely, the stagnant structure of the 100 nm-thick Al film (annealing times of 1-10 h), the 25 and 30 nm-thick Al films, and the fifteen Cu films. This distribution incorporates the size of 27,384 grains (out of the 30,639 measured). The distributions for individual samples are not shown, but they were found to be in close agreement.

The probability density for reduced area for two dimensional simulations with isotropic grain boundary energy is also given in Fig. 1. There is clear disagreement between experiment and simulation. Experiments show not only a larger population of smaller grains, but they also show grains with sizes that are much larger than the mean. In detail, simulations rarely see grains with areas larger than five times the mean, whereas the largest grains seen in the experimental structures range from as low as eight times the mean to as high as forty two times the mean. To discover the cause for the disagreement between experiments and simulations and for grain growth stagnation in the films, we examine the impact of various driving, retarding and pinning forces.

Surface Energy and Elastic Strain Energy:

In thin films, driving forces other than grain boundary energy reduction can promote the growth of grains. Examples include surface and elastic-strain energy driving forces. The minimization of these energies favors the growth of certain subpopulation of grains, and leads to the development of strong film texture.[4] However, for the 100 nm-thick Al films, the minimization of these energies should not have played a significant role in either the initial grain growth or the eventual stagnation since the films were very strongly $\langle 111 \rangle$ -fiber textured even in the as-deposited condition and annealing resulted in minimal strengthening of this texture.[5] In contrast to these Al films, the Cu films showed very weak textures. Despite this weak texture, the films had grain size distributions that

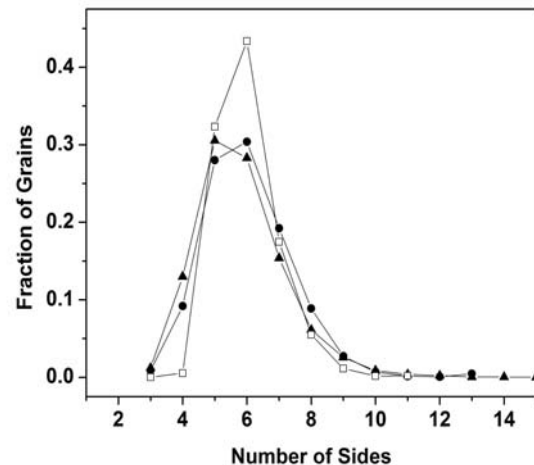


Fig. 2 - Distributions of the number of sides for the stagnant structure of the 100 nm-thick Al film (filled circles), two-dimensional simulations of normal grain growth with isotropic boundary energy (filled triangles), and simulation results (open squares) reported in [11] for pinning of grain boundaries by surface grooving for the case where $\kappa_{crit} = 0.4/\langle A_o \rangle^{1/2}$, where $\langle A_o \rangle$ is the mean grain area at the start of simulation.

were in very close agreement with those for the very strongly textured Al films. Thus, minimization of surface and elastic-strain energies should also not have played a significant role in the grain growth behavior of the Cu films either. Additionally, the Al and Cu film thicknesses studied here are below the thicknesses where elastic strain energy has been shown to significantly contribute to grain growth and texture evolution of thin films of face centered cubic metals.[4] Therefore, we conclude that surface and elastic strain energy reduction cannot explain the observed experimental results.

Anisotropy of Grain Boundary Energy: The anisotropic energy function listed in the experimental section reasonably approximates the Read-Shockley form for grain boundary energy as a function of misorientation. However, the simulation results for anisotropic grain boundary energy are not in better agreement with the experimental results when compared with the results for isotropic boundary energy, as seen in Fig. 1. Thus, we conclude that anisotropy of grain boundary energy cannot explain the experimentally observed stagnation of growth.

Grain Boundary Grooving: The formation of grooves and the resultant pinning of the boundaries by the grooves were first used by Mullins to explain stagnation of grain growth in thin metal foils.[8] In their work on thin film grain growth, Frost et al. [9] simplified Mullins' analysis by assuming that the critical curvature for boundary pinning was the same as that for escape from pinning. The analysis lead to a critical in-plane curvature, κ_{crit} , below which the boundary was pinned and became immobile. In their two-dimensional simulations, the grain boundary velocity was set to zero if the magnitude of the local curvature fell below κ_{crit} . As the simulation progressed, more and more boundaries became immobile and grain growth stagnated. The raw grain area data from Frost et al.'s simulations are not available to the authors, and, as a result, it is not possible to compare their results directly with the probability densities shown in Fig. 1. However, the grain size distribution for the stagnant structure in their simulations was found to be lognormal, as seen in experiments. The standard deviation of 0.28 for simulations with isotropic boundary energy is notably smaller than for experiments. The latter are in the range 0.36-0.6.[10]

Where experimental results and simulation results of boundary grooving can be compared directly is the distribution of the number of sides. As seen in Fig. 2, the grooving that is implemented in Frost et al.'s simulations leads to a narrowing of the distribution, for the case of isotropic grain boundary energy. This narrowing is manifested as a large drop in the number fraction of four-sided grains in the stagnant structure and a large increase in the fraction of six sided grains when compared with experiments. Figure 2 shows that the experimental distribution is in closer agreement with the simulations of normal grain growth than with the grain boundary grooving model.

Using the class of neighbors metric (i.e., the average number of sides of the

nearest neighbors of grains with given number of sides) for comparison, experiments and two dimensional simulations of normal growth show a clustering in which few-sided grains are neighbored by grains with larger number of sides and vice-versa, i.e., a downward trend as a

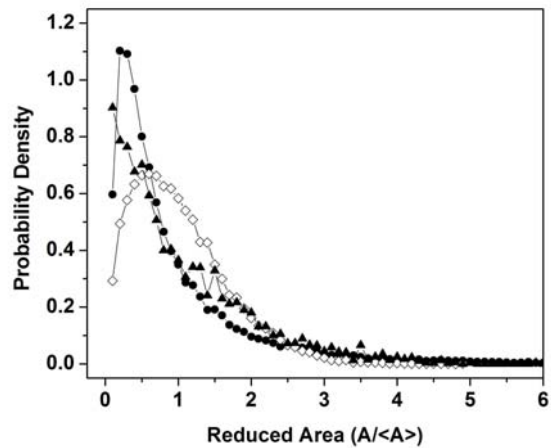


Fig. 3 - Probability densities for reduced area for experiment (filled circles) and two dimensional simulations of normal growth with isotropic boundary energy (open diamonds) given in Fig. 1 are compared with the results for two dimensional simulations of grain growth with triple junction drag (filled triangles). The drag parameter is 0.15 and is used here as an example of high of drag.

function of the number of sides. By contrast, grooving, as implemented in Frost et al.'s simulations, results in an opposite trend in clustering, wherein many-sided grains are neighbors of many-sided grains and few-sided grains are neighbors of few-sided grains.

In short, the three metrics of size, sides and class of neighbors show disagreement between experiments and the grooving model. Thus, we conclude that grooving cannot explain the observed experimental behavior.

Solute Drag: Solute drag has long been known as a mechanism for impeding the migration of grain boundaries, and, in cases where the solute content in the boundaries is high enough, grain growth can stop. To address the impact of solute drag on our experimental results in Al and Cu, we focus on the 100 nm-thick Al samples given that the purity of the Al sputtering target was significantly lower than the Cu sputtering target.

Gordon and El Bassayouni [12] studied grain growth in bulk samples of zone refined Al with Fe contents of 0.05 atomic ppm. They found that for annealing temperatures below 280 °C, grain growth ceased at a mean linear intercept size of 0.02 cm. Assuming that all the Fe atoms reside at the boundaries, the iron content of the boundaries for Gordon and El Bassayouni's bulk Al samples and for the stagnant structure of the 100 nm-thick Al film can be calculated.

The total number of Fe atoms in the 100 nm-thick Al film is calculated as $8.73 \times 10^{16} \text{ cm}^{-3}$ and that for the bulk Al sample of Gordon and El Bassayouni is calculated as $3.01 \times 10^{15} \text{ cm}^{-3}$. Using the total grain boundary areas per unit volume, the atomic surface density (choosing the {110} planes for simplicity) and the total number of Fe atoms in the samples, the surface atom content of Fe in the 100 nm thick samples is 848 atomic ppm (0.0848 at.%) and for the bulk Al sample of Gordon and El Bassayouni it is 34779 atomic ppm (3.48 at.%). Thus, the grain boundary surface atom fraction of Fe in the stagnant structure of the 100 nm-thick Al sample is more than 40 times lower than for bulk Al samples of Gordon and El Bassayouni. Furthermore, the cessation of grain growth in the bulk Al samples was only observed for annealing temperatures of 280 °C and below. Above this temperature, grain growth resumed again. Thus, given the significantly lower grain boundary Fe content and the significantly higher annealing temperature for the Al films, we conclude that solute drag alone cannot explain the observed stagnation of grain growth in these films. By extension, solute drag also cannot explain the grain growth behavior of the significantly purer Cu films.

Triple junction drag: Figure 3 compares the probability density of reduced area for experiments with those

for two dimensional simulations without and with triple junction drag at a high level of drag. Examination of the plots for all seventeen levels (not presented) shows that for the case of low drag, the probability density for reduced area is indistinguishable from the distribution for two dimensional normal growth with isotropic boundary energy. Increasing the level of drag simply depresses the peak in the distribution and replaces it with a decreasing probability density as a function of reduced size, as seen in Fig. 3.

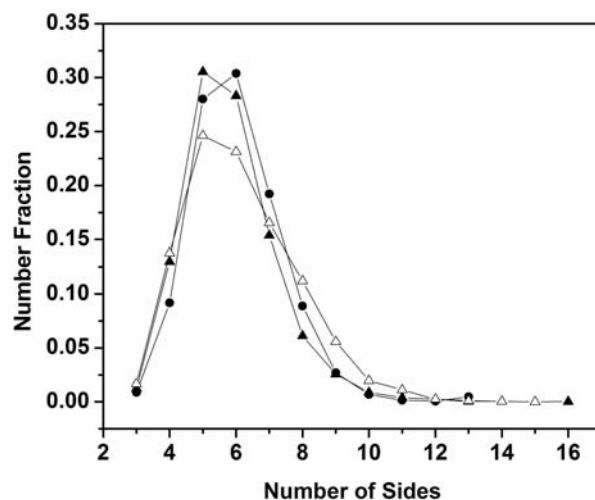


Fig. 4 - Comparison of the distributions for the number of sides for the stagnant structure of the 100 nm-thick Al film (filled circles), two dimensional simulations of normal grain growth with isotropic boundary energy (filled triangles), and simulations of grain growth with high triple junction drag (drag parameter of 0.15) (open triangles).

For the distribution of the number of sides, at low drag levels the distributions are indistinguishable from the simulation results for two dimensional normal growth with no drag. Agreement with experiment does not improve as the drag level is increased through the seventeen levels examined. The distributions become broader towards the higher number of sides as seen in Fig. 4 for the case of high drag.

In short, the two metrics of size and sides show disagreement between experiments and the grooving model at all the drag levels examined. Thus, we conclude that triple junction drag cannot explain the observed experimental results in the films.

Summary

In seeking an explanation for stagnation of grain growth in thin films and the cause of the differences between the experimental results and the results of two dimensional simulations of grain growth with isotropic boundary energy, we examined the impact of five factors. These were (i) surface and elastic strain energy, (ii) anisotropy of grain boundary energy, (iii) grain boundary grooving, (iv) impurity drag and (v) triple junction drag. No single factor was able to account for the experimental results. Thus, it is fair to say that a satisfactory explanation for stagnation of grain growth has not yet been found.

We gratefully acknowledge partial support from the MRSEC program of the NSF under DMR-0520425 and from the Semiconductor Research Corporation, Task 1292.008. We also thank D. Carpenter, G. Lucadamo, W. Archibald, V. Kumar, J. Kim, and A. King.

References

- [1] J. J. Thomson, Proceedings of the Cambridge Philosophical Society, Mathematical and Physical Sciences, Vol. 11 (1901), p. 120.
- [2] Information on <http://www.itrs.net/Links/2008ITRS/Home2008.htm>.
- [3] T. Sun, B. Yao, A. P. Warren, K. Barmak, M. F. Toney, R. E. Peale, and K. R. Coffey, Physical Review B, Vol. 79 (2009) p. 041402(R).
- [4] C. V. Thomson, Annual Review of Materials Science, Vol. 20 (1990), p. 245, and Vol. 30 (2000), p. 159, and Solid State Physics, Vol. 55 (2001) p. 269, and references therein.
- [5] K. Barmak, J. Kim, C.-S. Kim, W. E. Archibald, G. R. Rohrer, A. D. Rollett, D. Kinderlehrer, S. Ta'asan, H. Zhang, and D. J. Srolovitz, Scripta Materialia, Vol. 54, (2006) p.1059.
- [6] D. T. Carpenter, J. M. Rickman, and K. Barmak, Journal of Applied Physics Vol. 84 (1998) p. 5843.
- [7] D. Kinderlehrer, I. Livshits, and S. Ta'asan, SIAM Journal on Scientific Computation, Vol. 28 (2006) p. 1694.
- [8] W. W. Mullins, Journal of Applied Physics, Vol. 28 (1957) p. 333.
- [9] H. J. Frost, C. V. Thomson, and D. T. Walton, Acta Metallurgica et Materialia, Vol. 38 (1990) p. 1455.
- [10] See for example W. A. Archibald, Ph. D. Thesis, Carnegie Mellon University, Pittsburgh (2005).
- [11] S. P. Riege, C.V. Thompson, and H.J. Frost, Acta Materialia, Vol. 47 (1999) p. 1879 and references therein.
- [12] P. Gordon and T. A. El Bassayouni, Transactions of the Metallurgical Society of AIME, Vol. 233 (1965) p. 391.